# Analytical Seismic Fragility Analysis of Concrete Arch Dams


**X.W. Yao**
*Zhejiang University, China*

**A.S. Elnashai**
*University of Illinois at Urbana-Champaign, USA*

**J.Q. Jiang**
*Zhejiang University, China*

**SUMMARY:**
Concrete dams are critical structures, the failure of which would lead to catastrophic effects on a regional scale. Seismic fragility is used as a measure of the damage inflicted on a structure as a result of ground shaking. In this paper, seismic fragility analysis is applied to the safety evaluation of a concrete arch dam. A set of earthquake records were employed to present the variability in ground motion. Inelastic response-history analysis was used to analyze the three dimensional model of the high arch dam subjected to the suite of records scaled in terms of peak ground accelerations. The results show that the effects of earthquake records on dam deformation are substantial. The opening and slipping of contraction joints as well as the displacement at dam crest varies obviously with different records at varying peak ground acceleration levels.

*Keywords: high arch dam, fragility analysis, seismic response*

## 1. INTRODUCTION

Concrete dams bring enormous benefits in various aspects, such as flood control, power generation, and water diversion. However, the deterioration of high concrete dams to a large extent might result in the failure of dam structure. Consequently, a catastrophe may occur on the regional downstream area. In recent decades, several high concrete arch dams with heights of over 200 m have been completed in western China. However, some areas of dam locations are under the high risk of a seismic occurrence, which may give rise to an increasing awareness of the seismic damage on high arch dams. For instance, the Wenchuan (China) Earthquake in 2008 has brought a huge concern on the seismic safety of high dams near Wenchuan. Studies of the seismic risk on the safety of high dams have been funded by the Chinese government (Zhang, 2011).

Seismic fragility can be used as a measure of the damage inflicted on a structure resulting from an earthquake. Fragility is defined as the conditional probability when damage reaches or exceeds a specified level at varying ground shaking, e.g., peak ground parameters or spectral ordinates. As common and beneficial tools, fragility curves are adopted for the safety assessment of seismically vulnerable structures, such as buildings and bridges (Calvi et al., 2006; Padgett and DesRoches, 2008). Based on the sources of data, fragility curves can be categorized into four types (Rossetto and Elnashai, 2003), among which one approach uses numerical techniques to simulate the behaviour of structures, namely analytical fragility curves. An easy application to structures and geographical regions where in-situ seismic damage and earthquake records are insufficient makes analytical fragility curves widely and efficiently adopted (Nielson and DesRoches, 2007). For instance, the analytical fragility analysis is usually adopted in recent studies for the seismic fragility analysis of concrete gravity dams (Tekie and Ellingwood, 2002; Ghanaat et al., 2011). However, there is a dearth of fragility relationships for high arch dams due to limited field data and absence of efficient analytical approaches for conducting dynamic response history analyses of these structures. Of particular importance for fragility analysis of high arch dams is predicting the response of these structures to seismic actions as well as the relationship between the seismic input and the response of the structure. Unfortunately, previous

studies on seismic response of high arch dams, such as those done by Du and Tu (2007) and Zhong, Lin and Li (2008), are limited in considering the variation of input ground motions. For the reasons given above, there is the need for an improved understanding of the inelastic dynamic response of high arch dams subjected to realistic seismic records representative of near and far field earthquakes.

The purpose of this paper is to investigate the effect of various ground motions on seismic response of high arch dams. The three dimensional finite element model of a high arch dam was constructed, and 18 realistic earthquake records were selected and scaled to different intensity levels as input motions. Then, the seismic response of the high arch dam was obtained from inelastic response-history analysis. This paper focuses on the assessment of the opening and slipping of contraction joints as well as the displacement at the dam crest, and the effect of ground motions on the dam deformation is introduced. Because of space limitations, sample fragility relationships for high arch dams will be presented in companion papers.

## 2. METHODOLOGY

Fragility is the conditional probability of attainment or exceedance of the prescribed limit states for a chosen intensity measure of ground excitation, as shown in Eqn. 2.1.

$$P(\textit{fragility}) = P[LS \,|\, IM = x] \tag{2.1}$$

Where LS refers to limit state or the performance level, and IM represents the intensity measure of input ground seismic hazard with intensity level $x$. Fragility curves usually can be described by a lognormal cumulative distribution function (Ellingwood, 1990). However, there is no definitive method or strategy to construct fragility functions (Wen et al., 2003), especially when applied to comprehensive structures, such as dam structures.

Due to the various characteristics of ground motion, analytical models, structural materials, definition of limit states and so on, randomness and uncertainties generally exist on dam structures. This randomness and uncertainty can influence the seismic response of dams. Nevertheless, the time required to run the inelastic dynamic analysis for a three-dimensional (3-D) arch dam model is prohibitive if randomness and uncertainties are considered. Hence, for simplicity, only the variation of input ground motion is taken into account in this paper. The procedure for deriving analytically-based fragility curves for arch dams is presented as follows:

1) Generate an analytical model of concrete arch dams;
2) Select earthquake ground motion records which are applicable to the geographical area of interest;
3) Scale the PGA of the selected records to different excitation levels;
4) Perform inelastic dynamic response analyses using the scaled records;
5) Obtain the seismic responses of the dam model;
6) Compare the above results with the limit states predefined in the model;
7) Set up reasonable parameters which would be input into fragility curves;
8) Produce analytical fragility curves of concrete arch dams.

## 3. MODELING DESCRIPTION

The hydro complex is located in the southwestern part of China with the main function of electric power generation as well as the regulation of the seasonally high water discharges. The main parts of the complex are a reservoir, an arch dam, some outlet structures and a hydropower plant. The maximum height of this double curvature arch dam is 305 m with the crest elevation of 1885 m. The normal water level and dead water level of the reservoir are 1880 m and 1800 m, respectively. The maximum storage volume of the reservoir is about 7.77 billion $m^3$. The overall crest length of the dam

is 552.23 m, and the width is 13 m at the crest while 60 m at the base of the central cantilever. The arch dam consists of 26 monoliths divided by 25 vertical contraction joints. The peak value of the acceleration of the design basis earthquake is 0.197 g in the horizontal direction. The material properties for the concrete dam are shown as follows: unit weight is 2400 kg/m$^3$; Poisson's ratio and elastic modulus are 0.167 and 24 GPa, respectively; for the foundation rock: unit weight is 2700 kg/m$^3$; Poisson's ratio is 0.25; elastic modulus varies from 10 to 20 GPa for different elevations (see Table 3.1).

In this study, the software program ABAQUS is adopted to generate the numerical finite element model. As shown in Figure 3.1, the 3-D finite element dam-foundation system model has dimensions on *x*, *y*, *z* directions of 1270 m, 605 m and 1010 m respectively. An 8-node hexahedron element is used with the amount of 66015, and 105361 nodes are produced. For simplification, three vertical contraction joints are considered in the model. Their graphical layout is illustrated in Figure 3.2. Joint A is located in the middle of dam, while Joint B and Joint C are about 60 m apart on each side. A revised model of dynamic contact force is applied to simulate the non-linear contact between each contraction joint. The details of this contact model can be found in Yao, Jiang and Xu (2010). The dead water level is assumed as the water level in the reservoir, and the hydrodynamic pressure of the impounded water acting on the dam face is evaluated from the Westergaard's added mass formulae (Westergaard, 1933).

**Table 3.1.** Elastic modulus of foundation for decreasing elevations (GPa)

| Elevation (m) | 1885.0 | 1870.0 | 1830.0 | 1790.0 | 1750.0 | 1710.0 | 1670.0 | 1630.0 | 1600.0 | 1580.0 | Below 1580.0 |
|---|---|---|---|---|---|---|---|---|---|---|---|
| Left dam abutment | 10.0 | 10.0 | 10.0 | 12.0 | 12.0 | 12.0 | 11.0 | 11.0 | 19.0 | 19.0 | 15.0 |
| Right dam abutment | 10.0 | 15.0 | 20.0 | 20.0 | 20.0 | 20.0 | 20.0 | 14.0 | 14.0 | 11.0 | 15.0 |

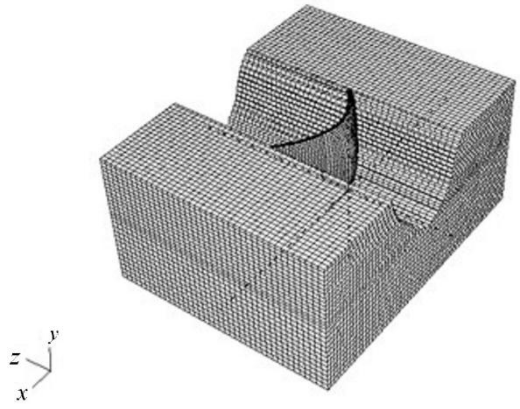


**Figure 3.1.** Finite element discrete model of dam-foundation system

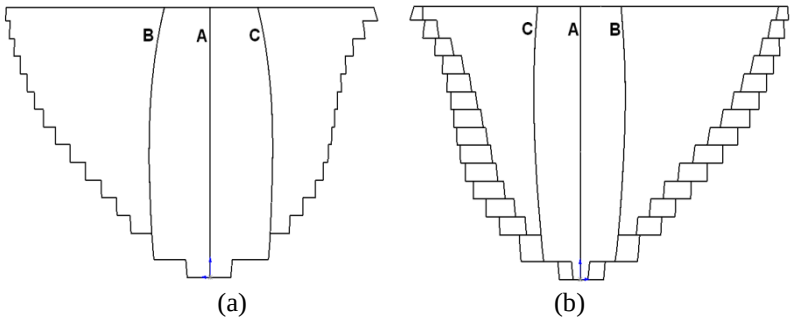


**Figure 3.2.** Layout of the contraction joints, (a) upstream surface, (b) downstream surface

## 4. SELECTION OF GROUND MOTION RECORDS

Since current studies focus on the effects of varying earthquake records on the seismic response of high arch dams, the records should be selected on the basis of various magnitudes and epicentral distances. Shome et al. (1998) stated that a suitable ensemble of ground motions for the purpose of analysis can be created by appropriate choices of records and scaling. Hence, 18 realistic ground motions are selected from the earthquakes around the world, as shown in Table 4.1. The records have epicentral distances (D) of 7.43 to 57.63 km with moment magnitudes ($M_w$) ranging from 5.1 to 7.6. The records are divided into three groups based on PGA. Taking the robustness of ground motions into consideration, PGA of the records are scaled to 0.1 g and 0.2 g for Group I, whereas for Group II and Group III it is 0.3 g to 0.5 g and 0.6 g to 0.8 g, respectively.

**Table 4.1.** Characteristics of the selected ground motions

| Record No. | Group No. | Earthquake | Date | Station | $M_w$ | D (km) | PGA (g) |
|---|---|---|---|---|---|---|---|
| 1 | I | Mammoth Lakes | 1980/05/25 | Long Valley Dam | 5.9 | 11.51 | 0.107 |
| 2 | | San Francisco | 1957/03/22 | Golden Gate Park | 5.3 | 11.13 | 0.112 |
| 3 | | Sierra Madre | 1991/06/28 | LA - City Terrace | 5.6 | 27.77 | 0.114 |
| 4 | | Northern California | 1975/06/07 | Cape Mendocino | 5.2 | 30.54 | 0.115 |
| 5 | | Whittier Narrows | 1987/10/01 | CIT Seis Sta | 6.0 | 19.56 | 0.123 |
| 6 | | Coalinga | 1983/05/09 | SGT (temp) | 5.1 | 7.43 | 0.139 |
| 7 | II | Northridge | 1994/01/17 | Santa Susana Ground | 6.7 | 14.66 | 0.29 |
| 8 | | Northridge | 1994/01/17 | LA - City Terrace | 6.7 | 39.15 | 0.316 |
| 9 | | Tabas | 1978/09/16 | Dayhook | 7.4 | 20.63 | 0.328 |
| 10 | | Hector Mine | 1999/10/16 | Hector | 7.1 | 26.53 | 0.337 |
| 11 | | Parkfield | 1966/06/28 | Temblor pre-1969 | 6.2 | 40.26 | 0.357 |
| 12 | | Loma Prieta | 1989/10/18 | Gilroy Array #1 | 6.9 | 28.64 | 0.411 |
| 13 | III | Northridge | 1994/01/17 | LA - Univ. Hospital | 6.7 | 36.47 | 0.493 |
| 14 | | Chi-Chi | 1999/09/20 | TCU088 | 7.6 | 57.63 | 0.508 |
| 15 | | Duzce | 1999/11/12 | Lamont 375 | 7.1 | 24.05 | 0.514 |
| 16 | | Landers | 1992/06/28 | Lucerne | 7.3 | 44.02 | 0.785 |
| 17 | | Tabas | 1978/09/16 | Tabas | 7.4 | 55.24 | 0.836 |
| 18 | | Cape Mendocino | 1992/04/25 | Cape Mendocino | 7.0 | 10.36 | 1.039 |

## 5. SEISMIC RESPONSE ANALYSIS

Inelastic response-history analysis is conducted to evaluate the seismic response of the high arch dam. This method is tedious but it is also the most direct way to assess the effect of ground motions on the seismic response of the structure. The 3-D finite element model of dam-foundation systems described above was subjected to each of the strong-motion records with different PGA levels. Previous studies show that opening, closure and slipping of contraction joints affect greatly the dynamic response of the arch dam subjected to earthquake ground motion (Fenves, Mojtahedi and Reimer, 1992; Zhang et al., 2000; Hu, Zhang and Lin, 2008). Hence, in this paper, the assessment of the seismic response of the high arch dam focuses on the slipping, opening of the contraction joints, as well as the deformation of the dam.

## 5.1. The slipping of joints

During the vibration of the arch dam due to the earthquake, the maximum slipping of joints usually occurs at the crest. Therefore, the assessment of maximum slipping for Joint A, Joint B and Joint C on upstream surfaces at the dam crest is introduced in this section. Table 5.1 shows the results of the maximum slippage at the crest and corresponding joints for each of the PGA intensity levels. It's obvious that the majority of the maximum slipping exists at Joint C. This can be explained by the structure of the arch dam model (see Figure 3.2), in which the right bank is much steeper than the left bank, and the monolith next to the right abutment is stiffer than the other monoliths.

It is also shown that for the same ground motion the increasing PGA levels cause more and more obvious slipping of the joints. However, the slipping of some records at medium intensity levels is much more pronounced relative to the slipping at high intensity levels. Based on the modelling analysis, it can be concluded that the seismic response of an arch dam is affected not only by the PGA of the ground motion but also by other intensity measures, e.g., spectral acceleration and spectral displacement. It also should be noted that the slipping of some records is extremely large while some slippage is too small to be noticed. The variability of the results may result from the uncertainty of different ground motions.

**Table 5.1.** The maximum slippage at joint crests (m)

| PGA / No. | 0.1 g | 0.2 g | PGA / No. | 0.3 g | 0.4 g | 0.5 g | PGA / No. | 0.6 g | 0.7 g | 0.8 g |
|---|---|---|---|---|---|---|---|---|---|---|
| 1 | 0.023 C | 0.024 C | 7 | 0.072 C | 0.137 C | 0.252 C | 13 | 0.138 C | 0.153 C | 0.161 C |
| 2 | 0.005 C | 0.005 C | 8 | 0.030 B | 0.054 C | 0.080 C | 14 | 0.037 C | 0.043 C | 0.055 C |
| 3 | 0.005 C | 0.025 C | 9 | 0.065 C | 0.110 C | 0.153 C | 15 | 0.029 C | 0.040 C | 0.049 C |
| 4 | 0.026 C | 0.026 C | 10 | 0.211 C | 0.543 B | 1.325 C | 16 | 0.025 C | 0.035 C | 0.046 C |
| 5 | 0.027 C | 0.028 C | 11 | 0.033 C | 0.036 C | 0.062 C | 17 | 0.943 C | 1.733 A | 3.673 C |
| 6 | 0.005 C | 0.027 C | 12 | 0.035 C | 0.058 C | 0.089 C | 18 | 0.058 C | 0.081 C | 0.121 C |

## 5.2. The opening of joints

This section presents the joint opening of the three joints on the upstream surface at the dam crest. Table 5.2 represents the maximum opening and the corresponding joint for different intensity levels. It is shown that the variability of the location for maximum opening is more pronounced at the higher intensity levels, which is quite different from that of maximum slipping. In addition, the locations of the maximum opening varied as the PGA level increases even for the same ground motion. It can be concluded that the opening of contraction joints is more sensitive to the characteristic of ground motion compared with the slipping. It is also interesting to observe that for the same ground motion the maximum opening increases when the PGA is scaled up even if it happens at different joints. Furthermore, ground motions can cause significant discrepancies in joint opening for the same location, even in the cases where the same intensity level is considered.

Fig. 5.1 shows the opening time-history at the top of joints. The results of record No. 11 at different intensity levels are shown to illustrate the variation of joint opening. As seen in Fig. 5.1, the opening displacements are quite different for Joint A, Joint B and Joint C as the PGA levels increase. In addition, the duration for the joint opening is observed for all these joints.

**Table 5.2.** The maximum opening at joint crests (m)

| PGA / No. | 0.1 g | 0.2 g | PGA / No. | 0.3 g | 0.4 g | 0.5 g | PGA / No. | 0.6 g | 0.7 g | 0.8 g |
|---|---|---|---|---|---|---|---|---|---|---|
| 1 | 0.000 C | 0.003 B | 7 | 0.032 B | 0.061 B | 0.094 B | 13 | 0.044 B | 0.061 B | 0.085 B |
| 2 | 0.000 C | 0.000 C | 8 | 0.008 A | 0.013 A | 0.025 B | 14 | 0.006 B | 0.009 C | 0.014 C |
| 3 | 0.000 C | 0.001 A | 9 | 0.021 B | 0.041 B | 0.063 B | 15 | 0.018 A | 0.022 A | 0.025 A |
| 4 | 0.000 C | 0.000 C | 10 | 0.082 B | 0.207 C | 0.418 C | 16 | 0.003 A | 0.005 A | 0.008 C |
| 5 | 0.000 C | 0.000 C | 11 | 0.010 A | 0.017 A | 0.022 A | 17 | 0.279 C | 0.487 B | 0.876 C |
| 6 | 0.000 C | 0.000 C | 12 | 0.008 A | 0.015 A | 0.020 A | 18 | 0.016 C | 0.032 C | 0.060 C |

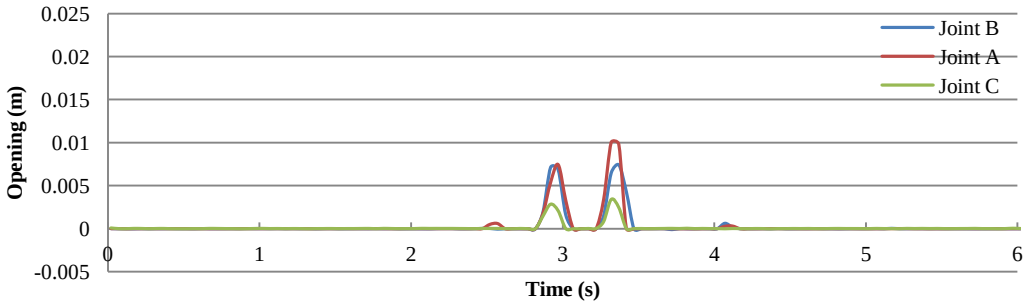


(a)

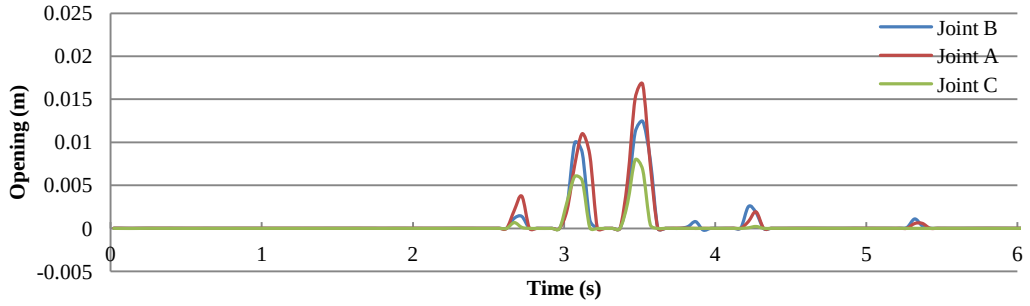


(b)

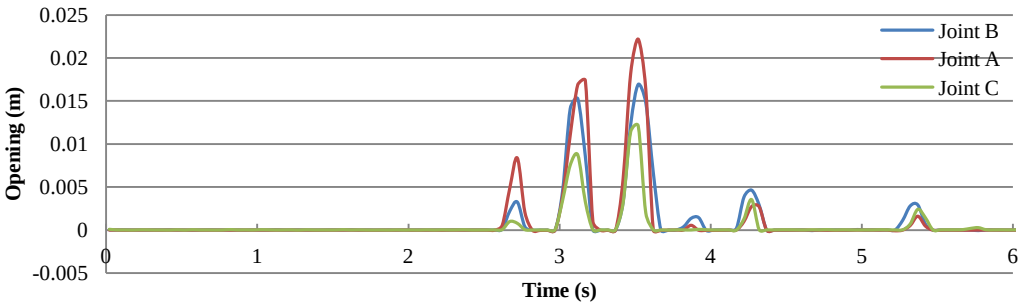


(c)

**Figure 5.1.** Joint opening time history for record No. 11 with different PGA levels: (a) 0.3 g PGA; (b) 0.4 g PGA and (c) 0.5 g PGA

### 5.3. Relationship between the slipping and opening of the joint

The slipping and opening time histories at the crest of Joint A for record No. 11 are shown in Fig. 5.2. Compared to the opening time history, slipping lasts for a longer period and its residual remained several seconds after the earthquake stopped. Moreover, the opening of joints was always accompanied by the occurrence of abrupt change of slipping; nevertheless, the maximum opening in most cases didn't synchronize with the maximum slipping.

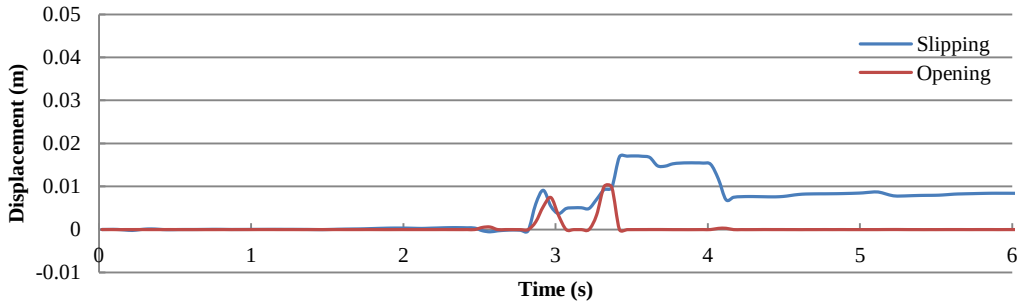


(a)

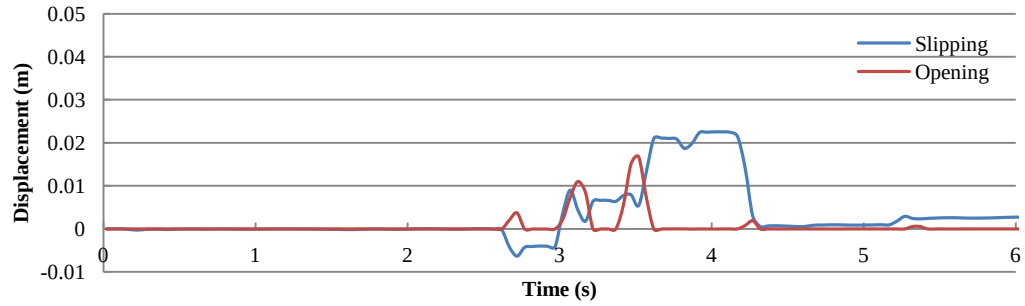


(b)

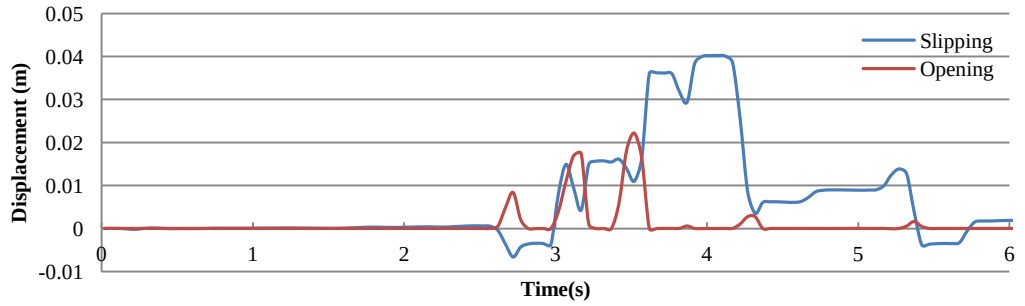


(c)

**Figure 5.2.** Opening and slipping time history of Joint A for record No. 11 with different PGA levels: (a) 0.3 g PGA; (b) 0.4 g PGA and (c) 0.5 g PGA

### 5.4. The relative displacement

In this section, the stream displacement of the crest of Joint A relative to the foundation is assessed. The arch dam moved upstream most of the time, which may be due to the fact that the reservoir kept in the dead water level. The relative displacement for the two sides of the crest of Joint A, indicated as Node 1 and Node 2, are monitored and assessed. It seems that Node 1 and Node 2 usually moved together for the first several seconds, followed by the difference in the relative displacement. The time

histories of the relative displacement at the top of dam for record No. 13 with different PGA levels are illustrated in Figure 3.3.

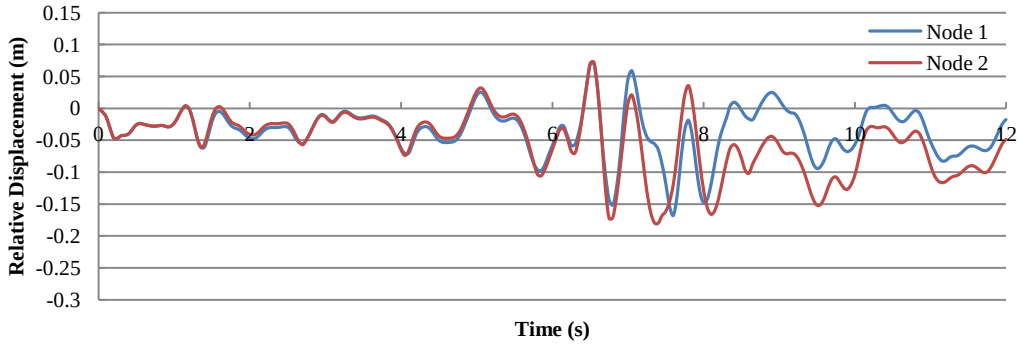


(a)

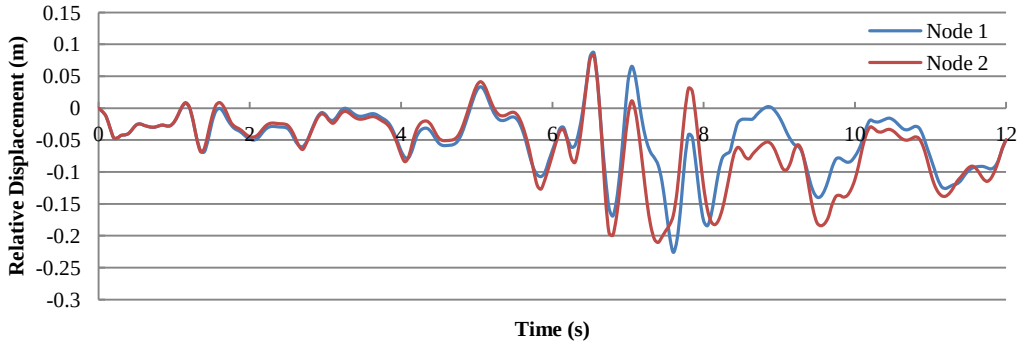


(b)

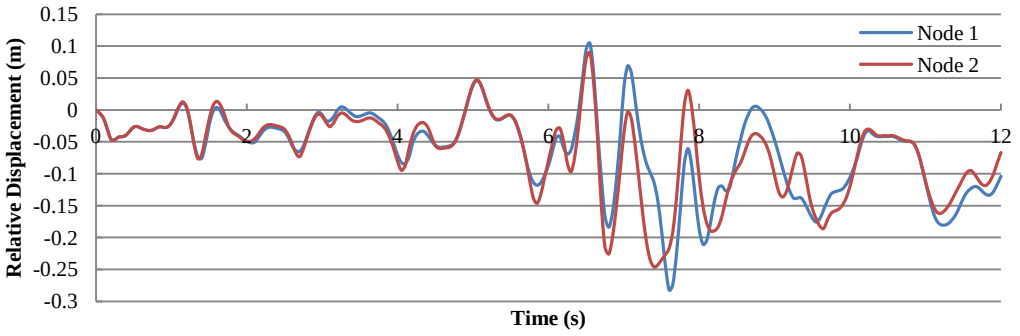


(c)

**Figure 3.3.** Relative displacement time history of Node 1 and Node 2 for record No. 13 with different PGA levels: (a) 0.6 g PGA; (b) 0.7 g PGA and (c) 0.8 g PGA

## 6. CONCLUSION

The purpose of this study is to assess the seismic response of arch dams subjected to earthquakes, and derive analytical fragility functions. A 305-meter-high arch dam is modelled using 3-D finite element models for inelastic response-history analysis. In order to assess the effects of various ground motions on the seismic response of the arch dam, 18 earthquake records with varying magnitudes and epicentral distances are selected and then scaled to different PGA levels as an input for the dam model. Results show that the majority of the obtained maximum slipping at the crest of joints occurred at Joint C which is close to the right dam abutment. However, the maximum opening happens variously

for different records, even for the same record but with different PGA levels. Furthermore, the seismic response at medium PGA levels are much more pronounced relative to that at high PGA levels, which indicates that the results of high arch dams are affected by several intensity measures, such as peak ground parameters, spectral acceleration and spectral displacement.

## REFERENCES


Calvi, G. M., Pinho, R., Magenes, G., Bommer, J. J., Restrepo-Velez, L. F. and Crowley, H. (2006). Development of seismic vulnerability assessment methodologies over the past 30 years. *ISET Journal of Earthquake Technology* **43:3**,75-104.

Du, X. L. and Tu, J. (2007). Nonlinear seismic response analysis of arch dam-foundation systems- part II opening and closing contact joints. *Bulletin of Earthquake Engineering* **5:**121-133.

Ellingwood, B. (1990). Validation studies of seismic PRAs. *Nuclear Engineering and Design* **123:2-3**,189-196.

Fenves, G. L., Mojtahedi, S. and Reimer, R. B. (1992). Effect of contraction joints on earthquake response of an arch dam. *Journal of structural engineering* **118:4**,1039-1055.

Ghanaat, Y., Hashimoto, P. S., Zuchuat, O. and Kennedy, R. P. (2011). Seismic fragility of Muhleberg dam using nonlinear analysis with latin hypercube simulation. *31st Annual USSD Conference*.1197-1212.

Hu, Z. Q., Zhang, D. and Lin, G. (2008). Effects of Joint-Movement on the Earthquake Response of Arch Dams. *14th World Conference on Earthquake Engineering*.

Nielson, B. G. and DesRoches, R. (2007). Seismic fragility methodology for highway bridges using a component level approach. *Earthquake Engineering & Structural Dynamics* **36:6**,823-839.

Padgett, J. E. and DesRoches, R. (2008). Methodology for the development of analytical fragility curves for retrofitted bridges. *Earthquake Engineering & Structural Dynamics* **37:8**,1157-1174.

Rossetto, T. and Elnashai, A. (2003). Derivation of vulnerability functions for European-type RC structures based on observational data. *Engineering Structures* **25:10**,1241-1263.

Shome, N., Cornell, C. A., Bazzurro, P. and Carballo, J. E. (1998). Earthquakes, records, and nonlinear responses. *Earthquake Spectra* **14:3**,469-500.

Tekie, P. B. and Ellingwood, B. R. (2002). Fragility Analysis of Concrete Gravity Dams. PhD thesis, The Johns Hopkins University, Baltimore.

Wen, Y. K., Ellingwood, B. R., Veneziano, D. and Bracci, J. (2003). Uncertainty modeling in earthquake engineering. Mid-America Earthquake Center Project FD-2 Report.

Westergaard, H. M. (1933). Water pressures on dams during earthquakes. *Transactions of the American Society of Civil Engineers* **98:2**,418-433.

Yao, X. W., Jiang, J. Q. and Xu, Y. K. (2010). Damage analysis of high arch dam including contraction joint and cracking nonlinearity. *Joint conference of 7CUEE&5ICEE.* 1789-1794.

Zhang, C. (2011). The performance of dams during the Wenchuan 5-12 earthquake and lessons learned from the event. *Journal of Earthquake and Tsunami* **5:4**,309-327.

Zhang, C. H., Xu, Y. J., Wang, G. L. and Jin, F. (2000). Non-linear seismic response of arch dams with contraction joint opening and joint reinforcements. *Earthquake Engineering and Structure Dynamics* **29:**1547-1566.

Zhong, H., Lin, G. and Li, H. J. (2008). Damage simulation of high arch dams in earthquakes. *14th World conference on earthquake engineering*.